

Figure 4-16. Changes in net current velocities (December 1996 to December 1997) in Central Bay caused by Scenario 1 (top) and Scenario 2 (bottom).

Figure 4-17 shows typical Suisun Bay peak flood (top) and ebb (bottom) mid-depth velocities for existing conditions from the SELFE model.

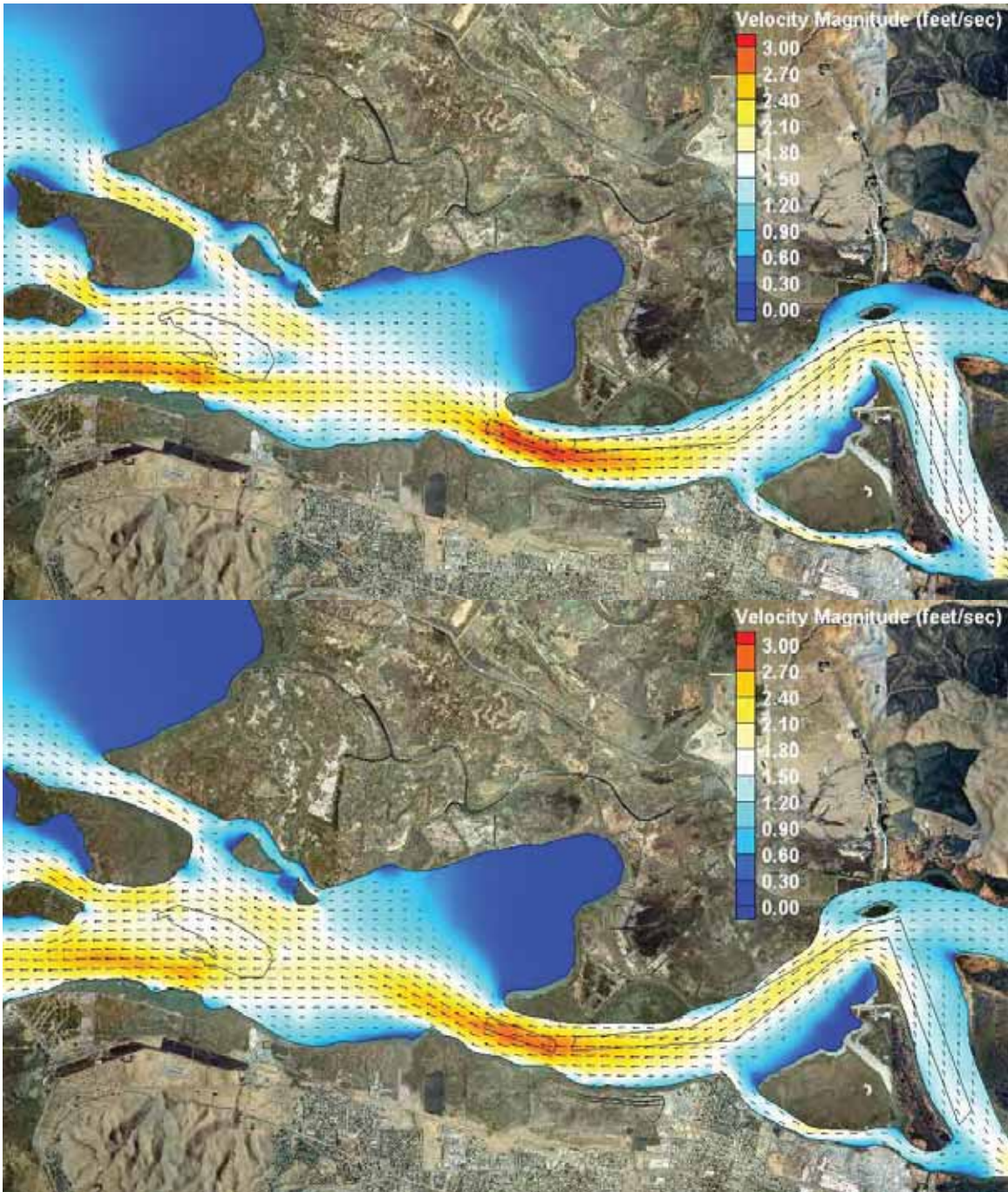


Figure 4-17. Typical flood (top) and ebb (right) mid-depth velocities in Suisun Bay for existing conditions

Current speed difference maps were also prepared for Suisun Bay. Figures 4-18 and 4-19 show mid-depth current speed differences in Suisun Bay caused by Scenarios 1 and 2, respectively, compared to existing conditions. Analysis indicates that in general the velocity patterns surrounding the lease areas are very similar between existing conditions, Scenario 1 and Scenario 2. Changes in mid-depth current speeds are less than approximately 0.5 feet/sec, even when measured over the most heavily

mined lease areas. Changes are not measurable away from the lease areas, generally at distances away from the lease areas that are similar to the sizes of the lease areas themselves.

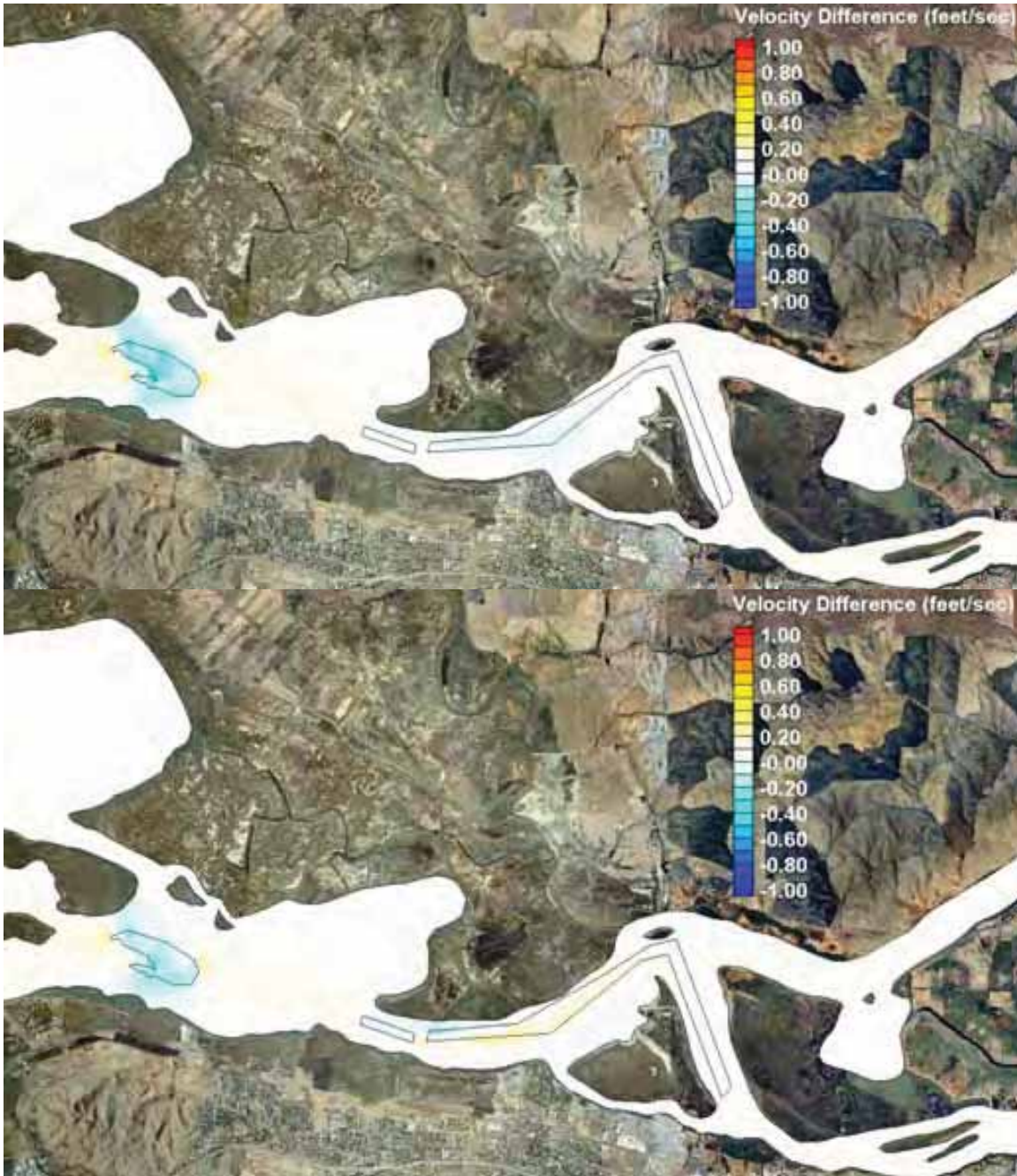


Figure 4-18. Mid-depth flood (top) and ebb (bottom) current speed differences in Suisun Bay caused by Scenario 1

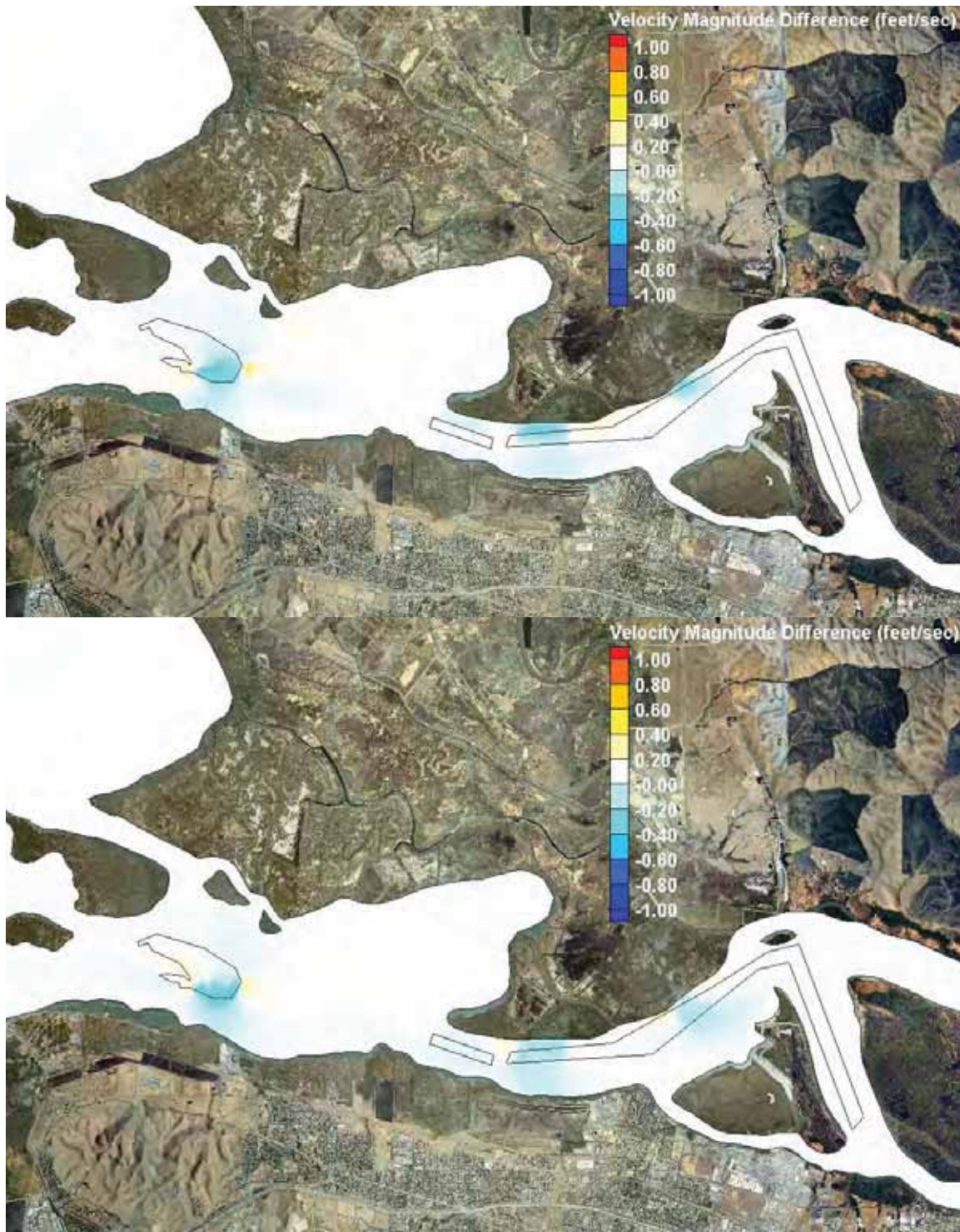


Figure 4-19. Mid-depth flood (top) and ebb (bottom) current speed differences in Suisun Bay caused by Scenario 2

A time series analysis of mid-depth velocities surrounding the lease areas was also performed at Points 22-41 shown in Figure 4-10. Figure 4-20 shows time histories of mid-depth velocity at Points 24 (left) and 29 (right) in Suisun Bay. The velocity time histories for existing conditions, Scenario 1 and Scenario 2 are almost

indistinguishable in the figure, indicating that bottom changes due to sand mining do not measurably change the overall current speed regime at these locations.

The maximum current speed difference present at any Suisun Bay analysis location (see Figure 4-10) for both alternatives was approximately 0.05 feet/sec. In general, the current speed differences caused by the sand mining at the locations used for analysis are not expected to be measurable.

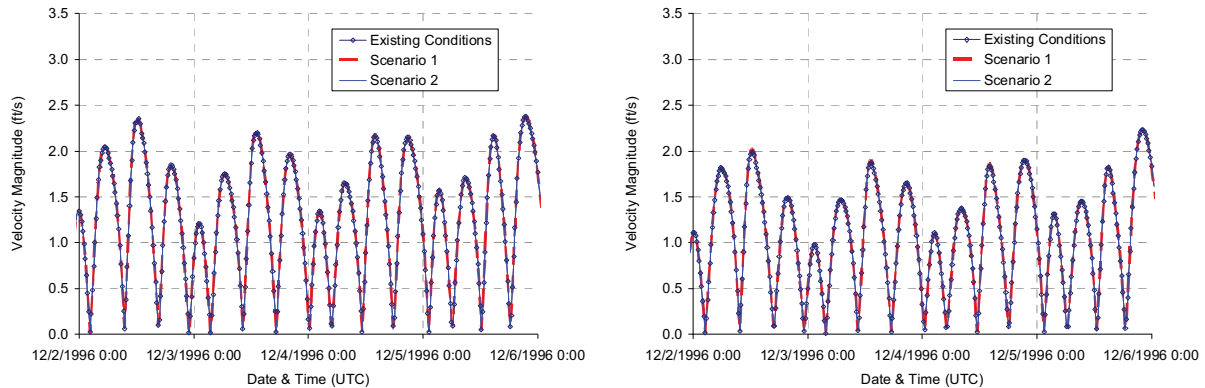


Figure 4-20. Mid-depth current speed at Point 24 (left) and Point 29 (right) for existing conditions, Scenario 1 and Scenario 2 (Point Locations in Figure 4-10)

Figure 4-21 shows the one-year net velocities for existing conditions in Suisun Bay. Figure 4-22 shows the changes in net velocities induced by Scenario 1 (top) and Scenario 2 (bottom). Suisun Bay net current velocities are much stronger than Central Bay net velocities in the lease areas due to the presence of unidirectional river discharge. Analysis indicates that the full-year net current velocities in Suisun Bay are not affected in areas outside the vicinity of the lease areas. The areas over which net flows are affected more than 0.05 feet/sec is approximately as large as the lease areas themselves.

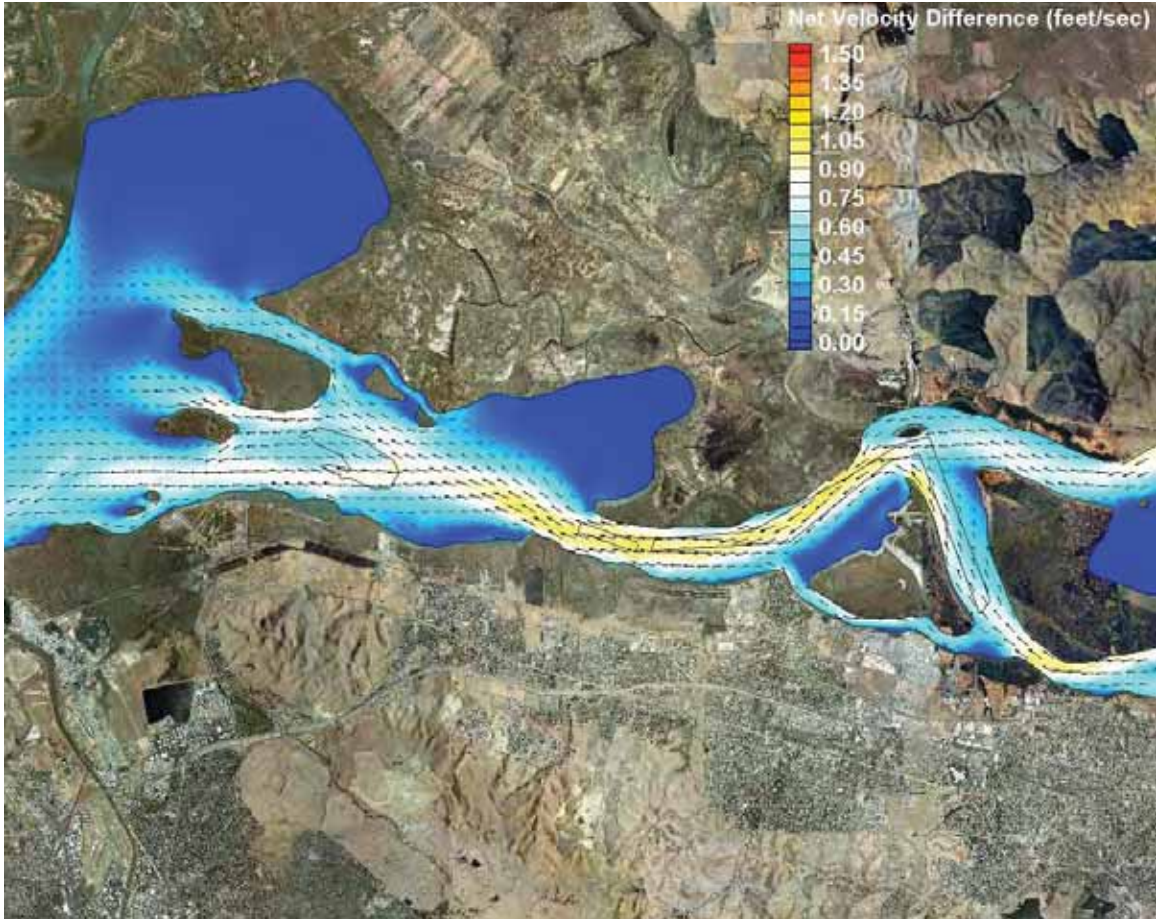


Figure 4-21. Net current velocities (December 1996 to December 1997) in Suisun Bay for existing conditions

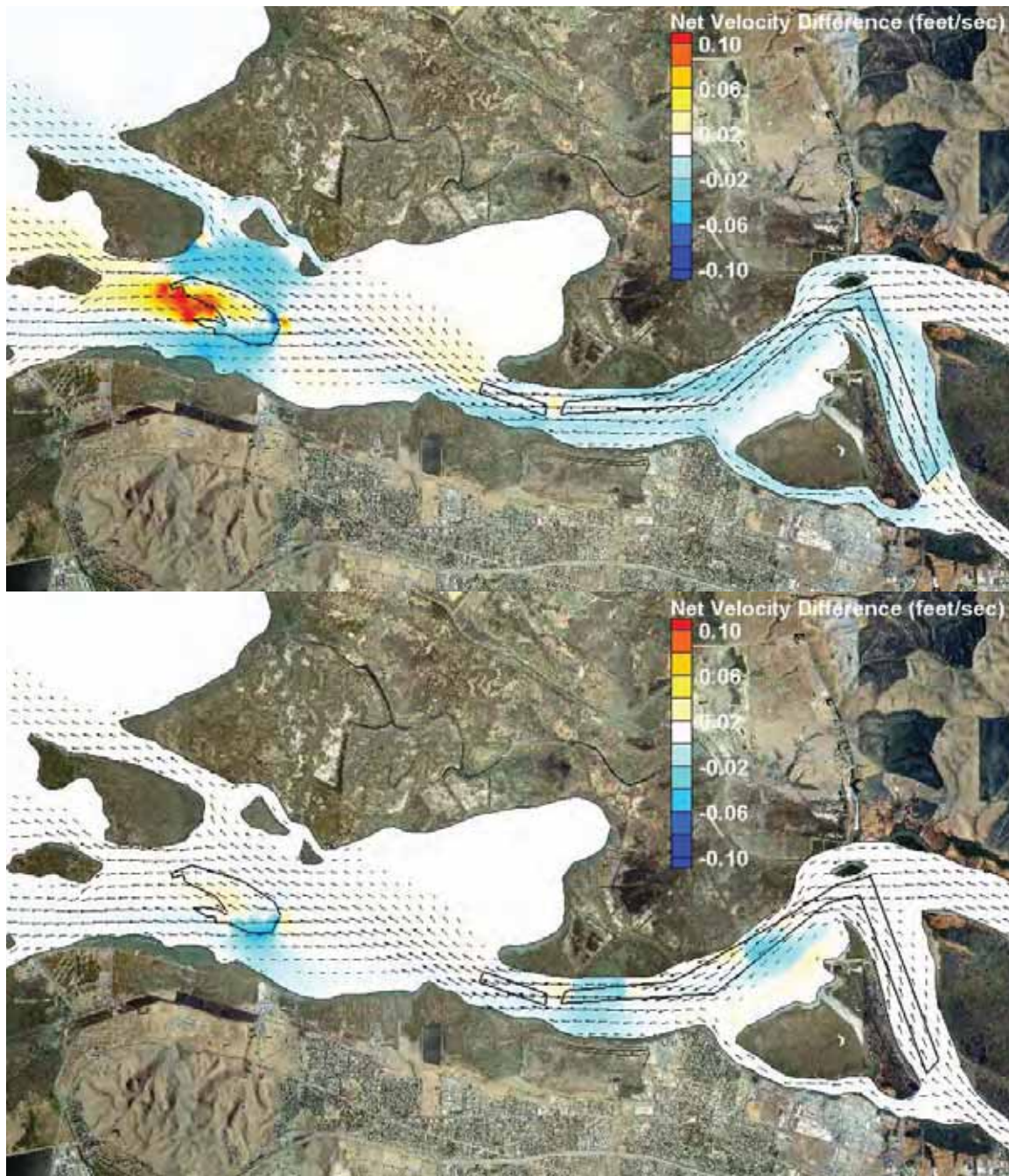


Figure 4-22. Changes in net current velocities (December 1996 to December 1997) in Suisun Bay caused by Scenario 1 (top) and Scenario 2 (bottom)

Circulation modeling results from both short-term and full-year simulations in both Central and Suisun Bays indicate that tidal and river current flows are not likely to be affected by the sand mining activities except in the vicinity of the mining areas. The vicinity of measurable changes is generally similar in size to the lease areas themselves.

4.2.5. Changes to Salinity due to Sand Mining

Salinity was also evaluated with the SELFE model within the short-term simulation to determine if the sand mining is likely to result in changes to the salinity patterns surrounding the project area. Figures 4-23 and 4-24 show plan views of bottom salinity for existing conditions during typical peak flood and ebb currents, respectively, in Central Bay. These two figures also each show vertical profiles of salinity during peak currents for existing and after-mining conditions.

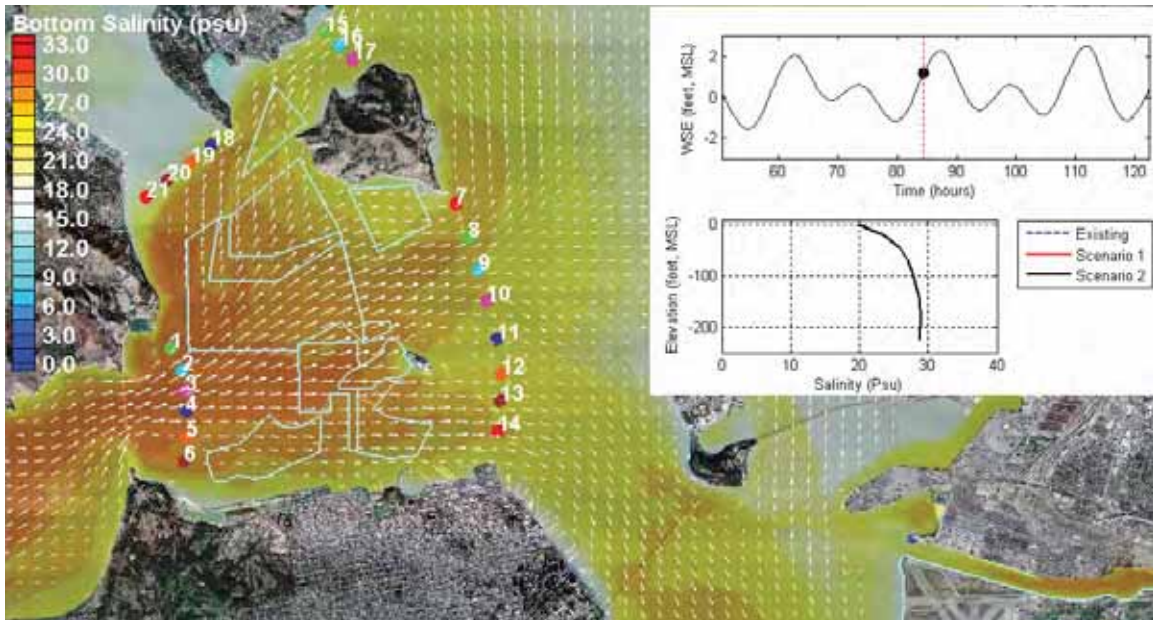


Figure 4-23. Bottom salinity (color contours) and vertical profiles of salinity at Point 4 in Central Bay for all scenarios during peak flood velocities

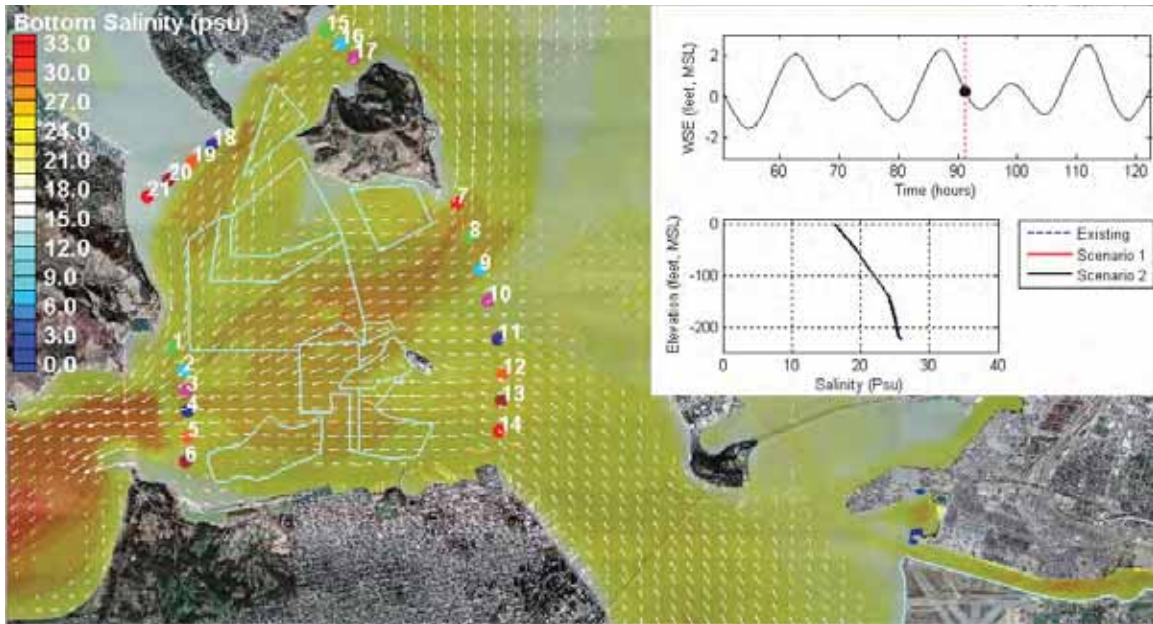


Figure 4-24. Bottom salinity (color contours) and vertical profiles of salinity at Point 4 in Central Bay for all scenarios during peak ebb velocities

Results indicate no measurable differences in salinity profiles at the locations used for analysis. However, at some times during the simulations, small salinity changes can be noticed in the near-bottom areas. The salinity differences are only temporary during periods of weaker currents (higher salinity in the mining holes), and salinity levels return to surrounding levels when stronger currents return. It should be noted that although care was taken to reasonably represent the dredging holes caused by mining, the system-wide scale of the analysis prevents highly detailed flow modeling surrounding the mining holes. Therefore, it should be expected that some slightly increased salinity levels could be present in the deeper holes if salinity levels are reduced in Central Bay from river discharge, particularly if Scenario 2 were put into practice (deepening up to 35 feet in some areas).

Salinity was also evaluated in Suisun Bay with the SELFE model. However, the salinity values measured by USGS (data that were used as initial conditions) were negligible in Suisun Bay. Since near-zero values existed in the modeling results a quantitative comparison was not made; however, results and conclusions similar to those from Central Bay should be expected for periods when salinity is higher in Suisun Bay.

Modeling results from the short-term salinity simulations indicate that salinity levels are not likely to be affected by the sand mining activities except during brief periods of time within the mining holes, where some small, short-term bottom salinity increases may occur, particularly for Scenario 2.

4.2.6. Changes to Sediment Transport due to Sand Mining

Numerical modeling of sand transport and bottom morphology for both short-term simulations (15 days) and full-year simulations (using December 1996 to December 1997 hydrologic/tide data input) was performed with the two-dimensional LAGRSED model (Maderich *et al.*, 2004). The LAGRSED model used hydrodynamics from the SELFE model as input. The sediment transport model description, setup, and input data are provided in Appendix D.

The LAGRSED model is a Lagrangian (particle-tracking) sediment transport model that computes suspended and bedload sediment transport fluxes and bed changes for a variety of sediment sizes distributed around the Bay. In order to best utilize the 3D hydrodynamic results, the shear stress values calculated by the SELFE model were input directly into the 2D LAGRSED model for calculation of transport rates and morphology. In the short-term simulations, patterns of sediment transport rates were compared to determine if any changes in hydrodynamics are likely to cause changes in instantaneous transport. Transport rates are highly variable due to the large variation in sediment sizes, highly variable pattern of near-bottom velocity and highly variable bathymetry.

Figure 4-25 shows Central Bay total sediment transport (bedload plus suspended load) during typical peak flood (top) and ebb (bottom) velocities for existing conditions. Figures 4-26 and 4-27 show changes in total transport relative to existing conditions for Scenarios 1 and 2, respectively, during typical flood (top) and ebb (bottom) currents. The color contours represent changes in total transport and vectors represent total transport for existing conditions. Total sediment transport time series were also extracted at the points shown in Figure 4-9 for all scenarios.

Figure 4-28 shows time histories of the total sediment transport rate (bedload plus suspended load) at the selected extraction points. Time histories at Points 4 and 10 in Central Bay show no measurable transport rate differences. Results indicate that total sediment transport is not likely to be measurably altered outside the immediate vicinity of the lease areas.

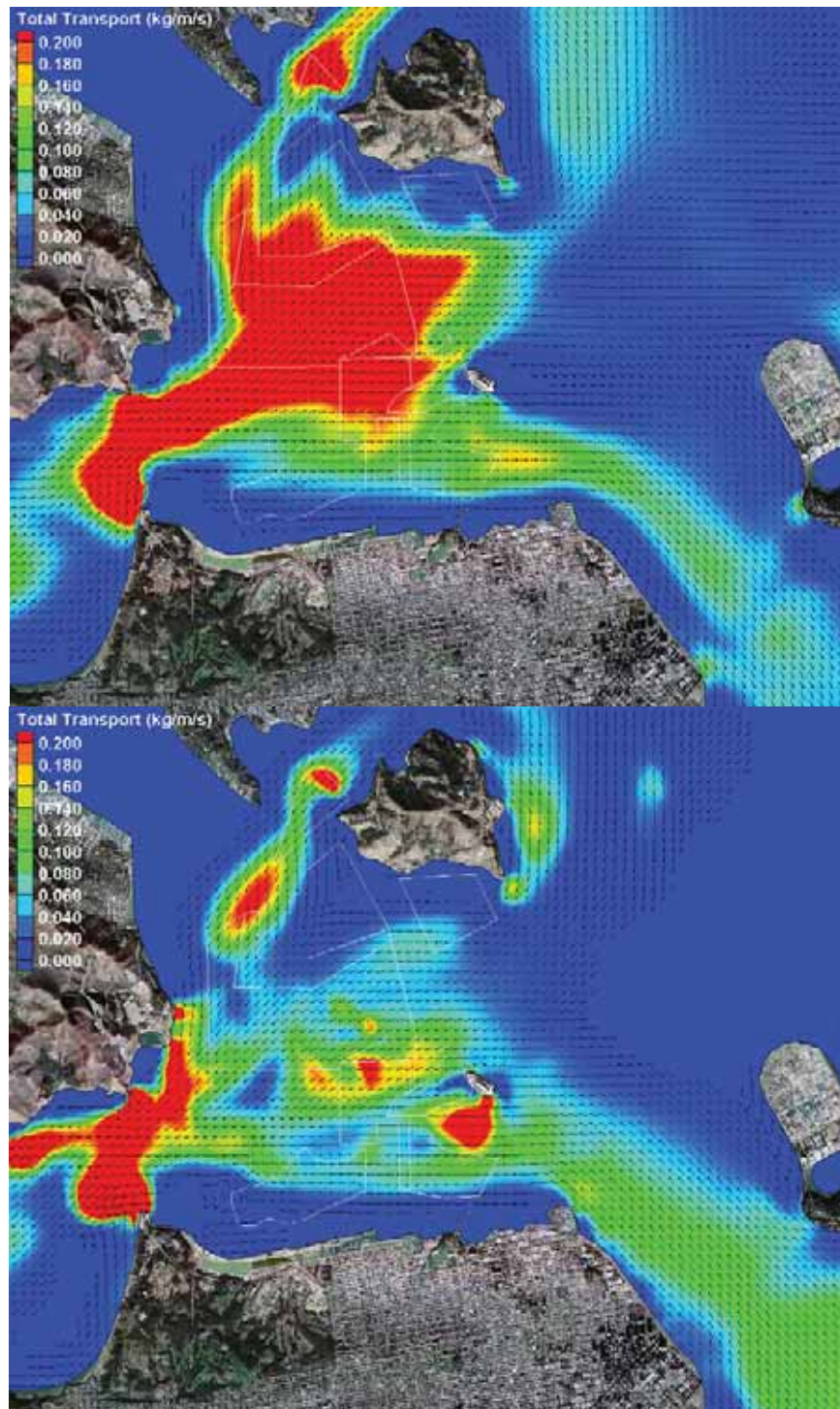


Figure 4-25. Total transport in Central Bay for existing conditions during typical flood (top) and ebb (bottom) currents

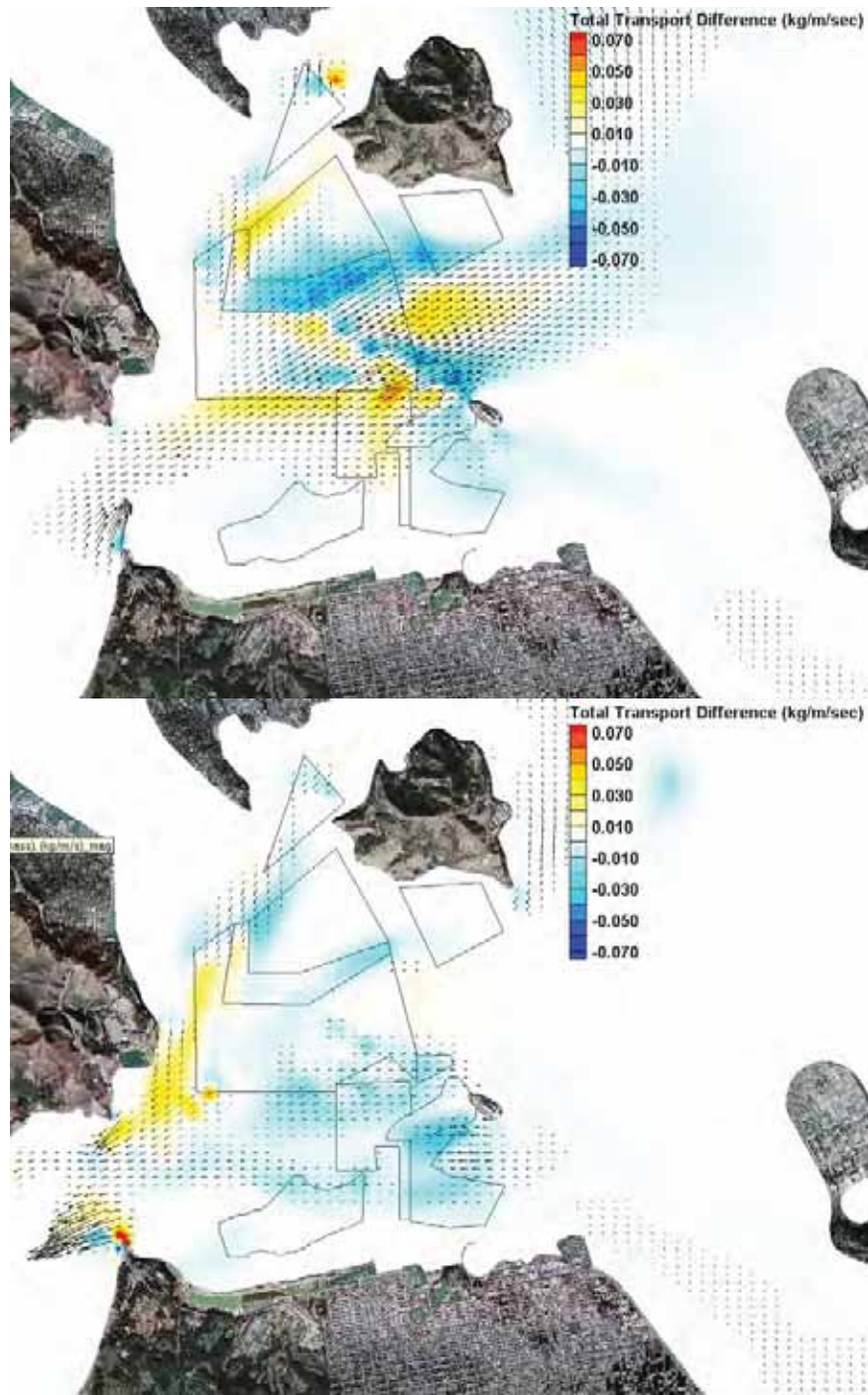


Figure 4-26. Scenario 1 changes in total transport in Central Bay for existing conditions during typical flood (top) and ebb (bottom) currents

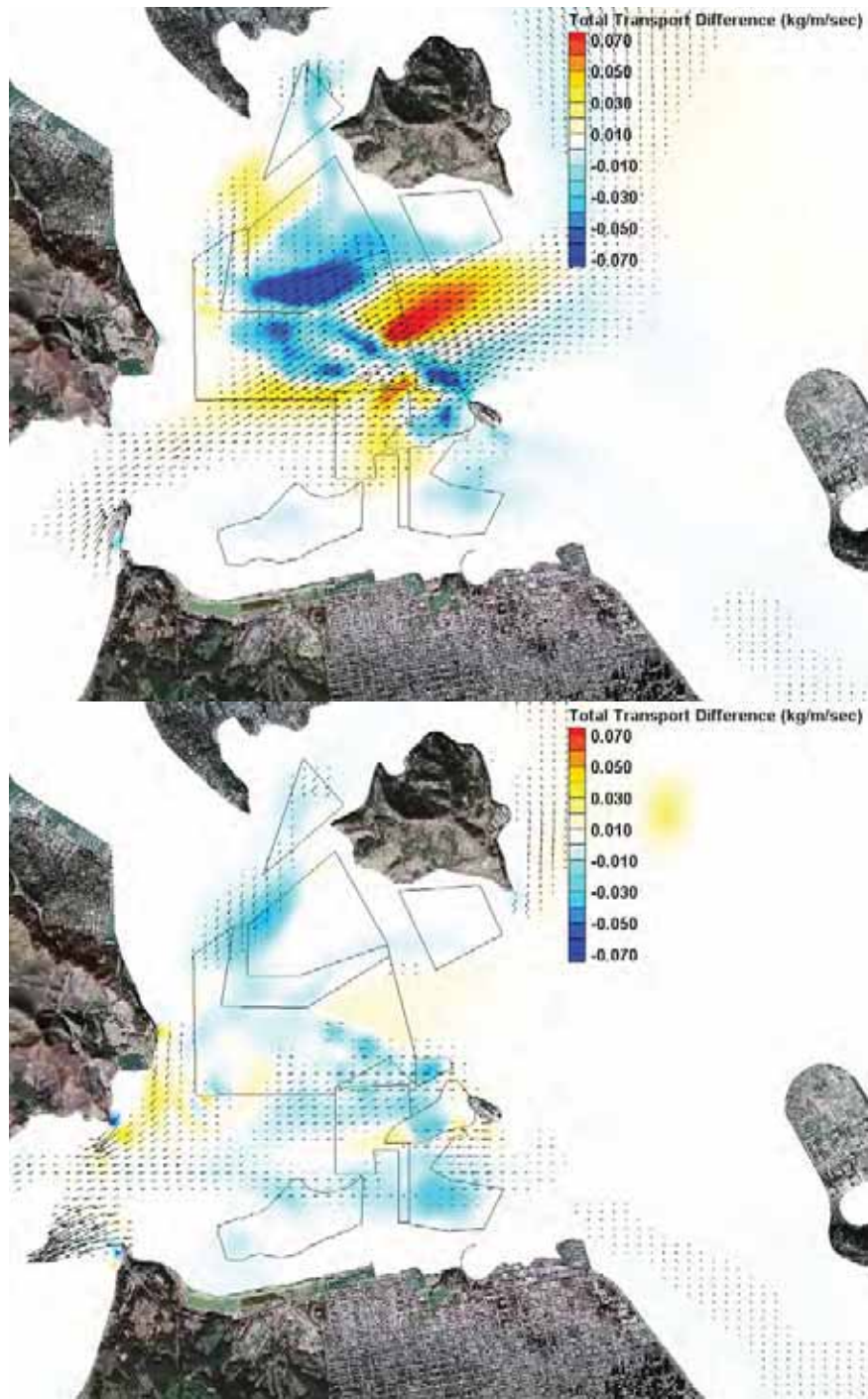


Figure 4-27. Scenario 2 changes in total transport in Central Bay for existing conditions during typical flood (top) and ebb (bottom) currents

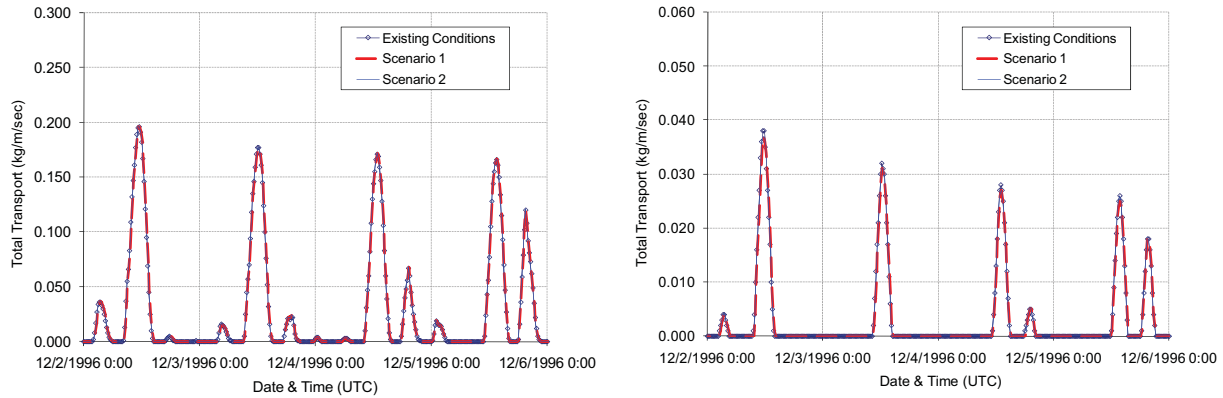


Figure 4-28. Time history of total transport at Points 4 (left) and 10 (right) in Central Bay

One-year sediment transport simulations were also performed using the LAGRSED model to capture high-flow effects. Figure 4-29 shows the net sediment transport from the one-year simulation for existing conditions in Central Bay. The net transport patterns are typically small except in areas that tend to have largely unidirectional flows, or a consistently large difference between ebb and flood current speeds.

Figures 4-30 and 4-31 show differences in net bedload sediment transport caused by sand mining relative to existing conditions for Scenarios 1 and 2, respectively. LAGRSED model results indicate that full-year (net) bedload sand transport patterns are not likely to be affected by the mining activities except in the vicinity of the mining areas. In areas farther than approximately the size of the lease areas, the changes are less than 5%.



Figure 4-29. Net bedload transport in Central Bay for existing conditions

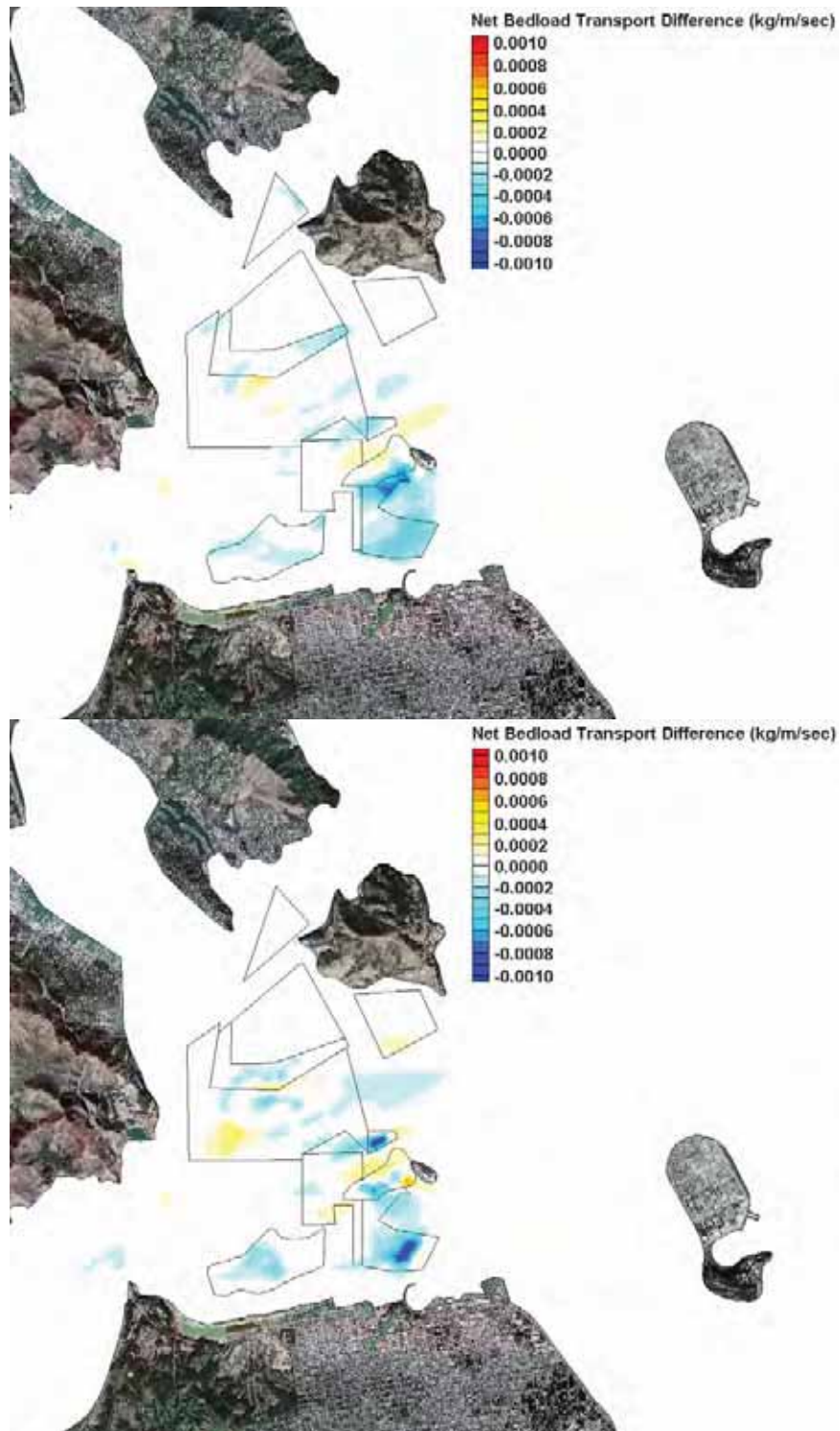


Figure 4-30. Scenario 1 (top) and Scenario 2 (bottom) changes in full-year net bedload transport in Central Bay

Figure 4-31 shows upper Suisun Bay total sediment transport (bedload plus suspended load) during typical peak flood (top) and ebb (bottom) velocities for

existing conditions during the short-term simulation. Figures 4-32 and 4-33 show changes in total transport relative to existing conditions for Scenarios 1 and 2, respectively, during typical flood (top) and ebb (bottom) currents.

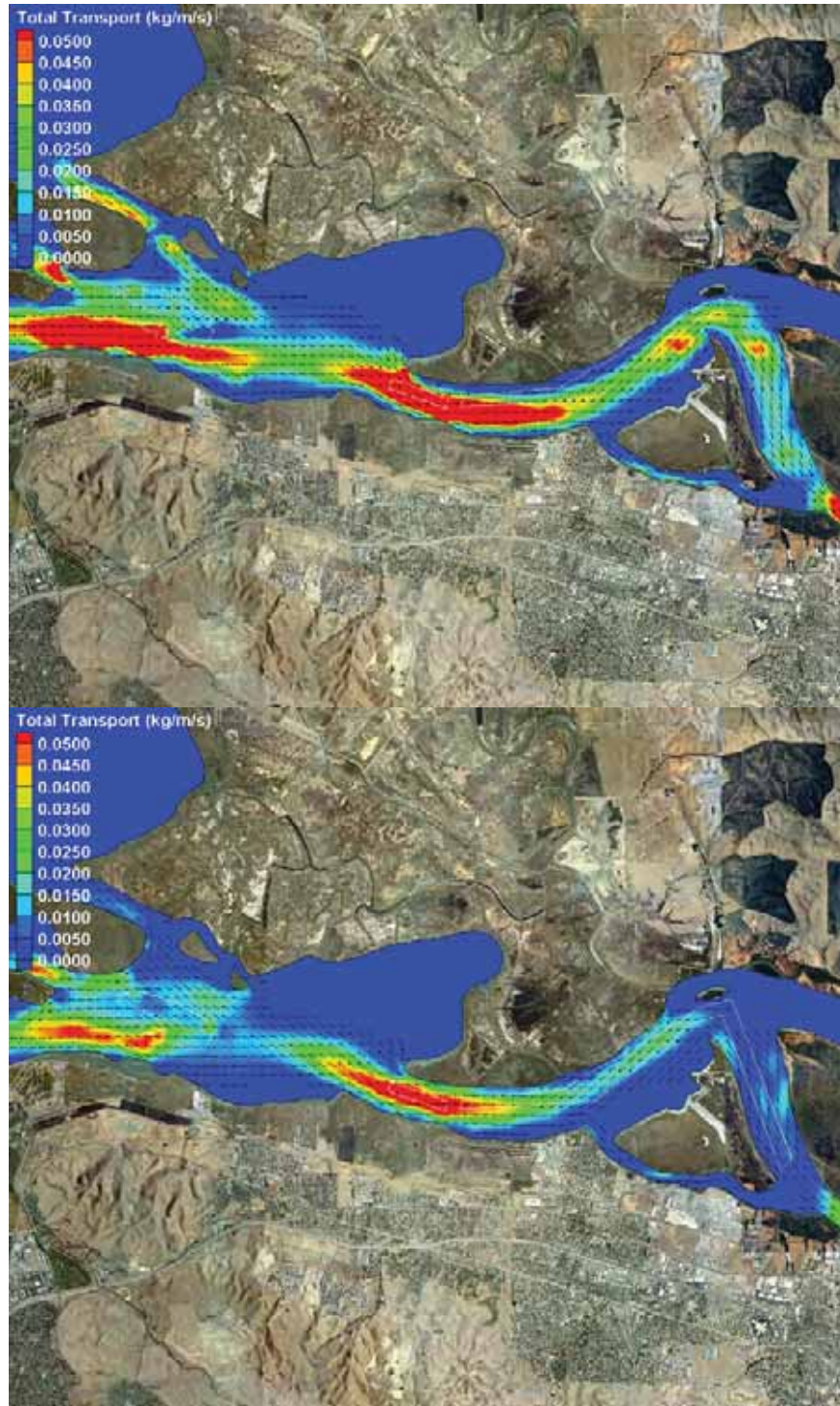


Figure 4-31. Total sediment transport in Suisun Bay for existing conditions during typical flood (top) and ebb (bottom) currents

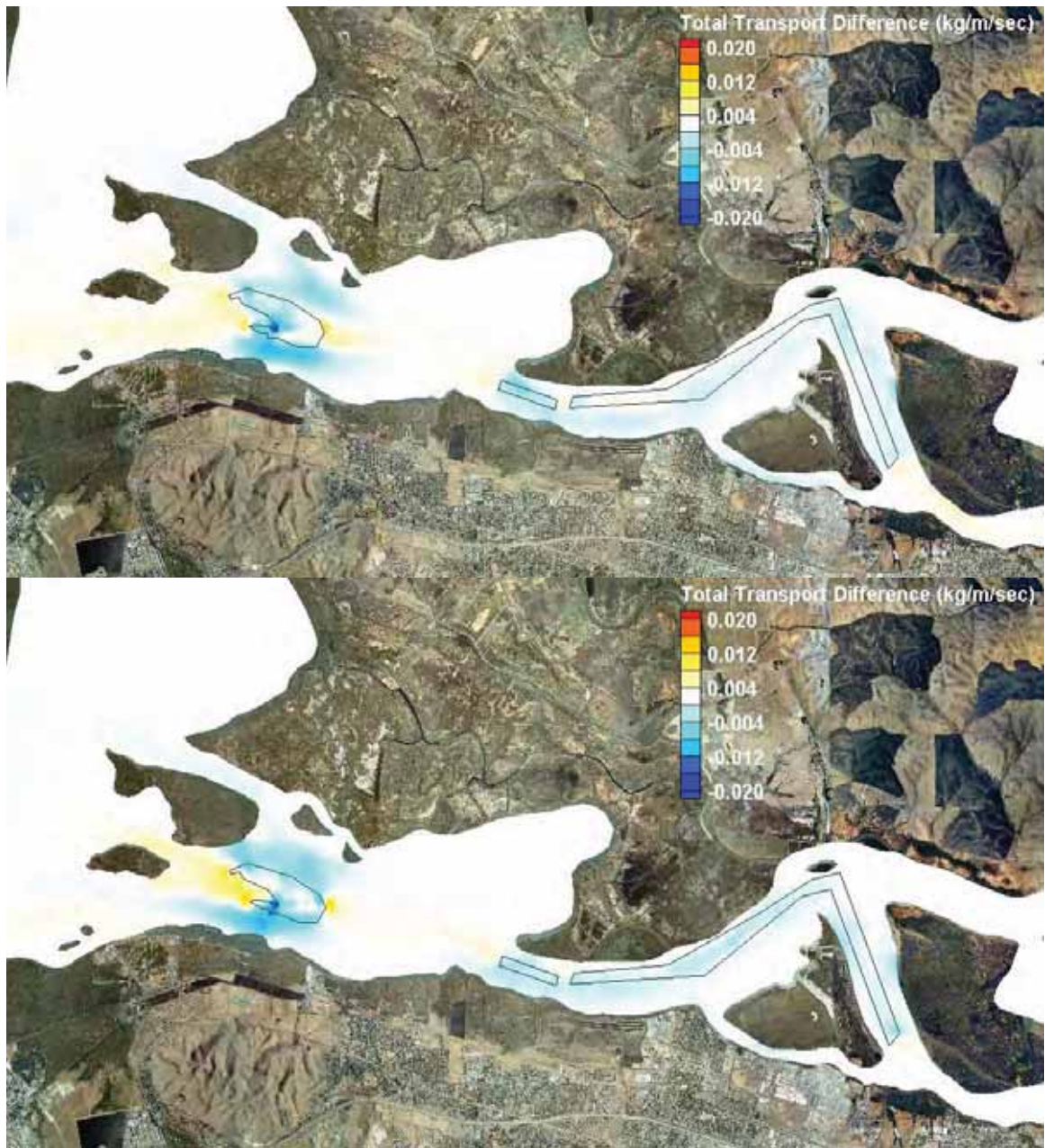


Figure 4-32. Scenario 1 changes in total transport in Suisun Bay for existing conditions during typical flood (top) and ebb (bottom) currents

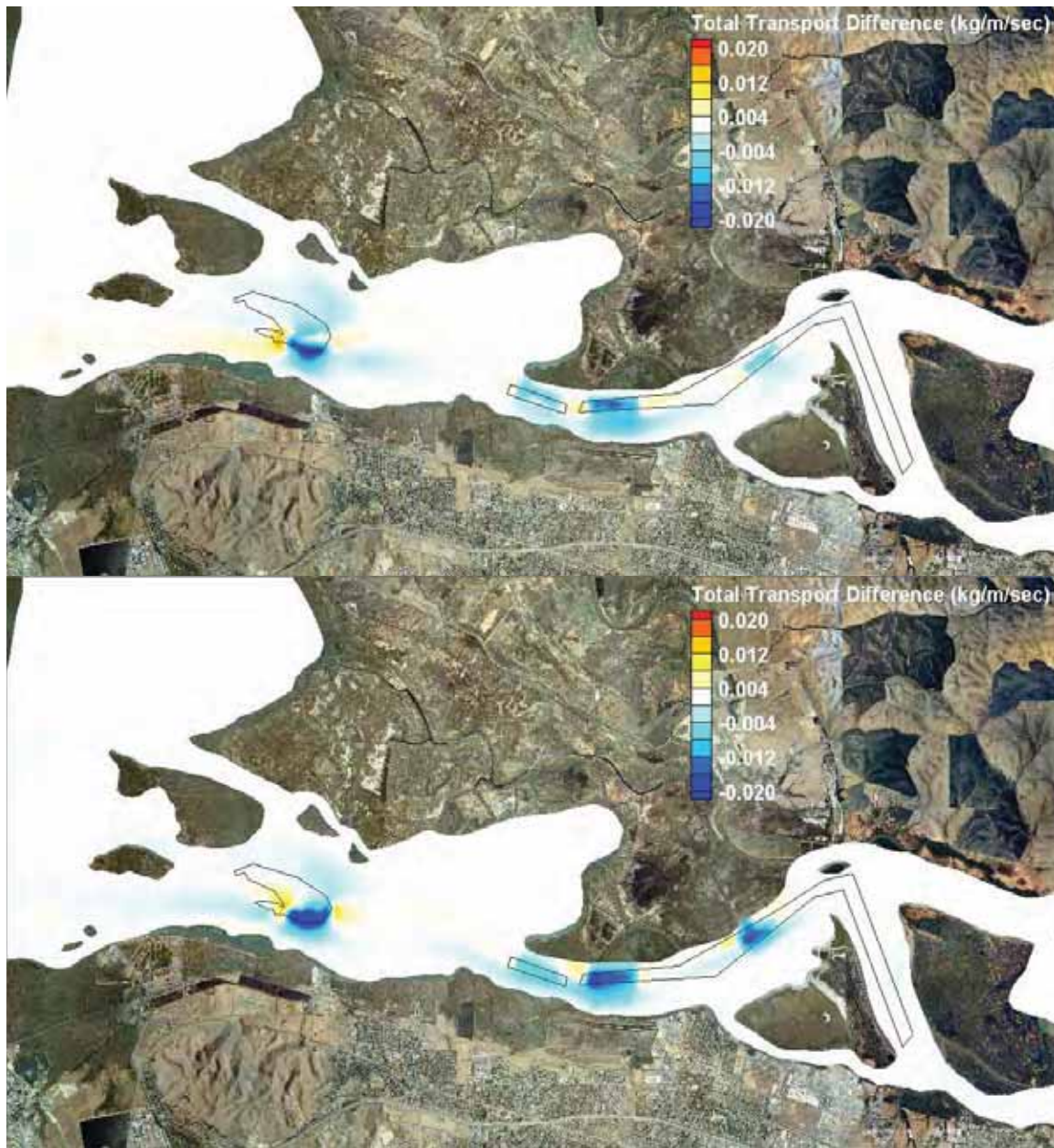


Figure 4-33. Scenario 2 changes in total transport in Suisun Bay for existing conditions during typical flood (top) and ebb (bottom) currents

A total sediment transport time series was also extracted at the points shown in Figure 4-11 for all scenarios. Figure 4-34 shows time histories of the total sediment transport rate (bedload plus suspended load) at the selected extraction points. Time histories at Points 24 and 29 in Suisun Bay show no measurable transport rate differences.

Figure 4-35 shows the net bedload sand transport from the one-year simulation for existing conditions. Figure 4-36 shows the differences in net bedload sand transport